Glucometabolic consequences of acute and prolonged inhibition of fatty acid oxidation[S]

Anne-Marie Lundsgaard,* Andreas M. Fritzen,* Trine S. Nicolaisen,* Christian S. Carl,* Kim A. Sjøberg,* Steffen H. Raun,* Anders B. Klein,† Eva Sanchez-Quant,§ Jakob Langer,§ Cathrine Ørskov, Christoffer Clemmensen,† Matthias H. Tschöp,§,††,§§ Erik A. Richter,* Bente Kiens,[1],* and Maximilian Kleinert[1],*,§**

Section of Molecular Physiology,* Department of Nutrition, Exercise, and Sports, Faculty of Science, University of Copenhagen, Copenhagen, Denmark; Institute for Diabetes and Obesity,§ Helmholtz Diabetes Center at Helmholtz Zentrum München, German Research Center for Environmental Health, Neuherberg, Germany; Department of Biomedical Sciences** and Novo Nordisk Foundation Center for Basic Metabolic Research,† Faculty of Health and Medical Sciences, University of Copenhagen, Copenhagen, Denmark; German Center for Diabetes Research (DZD),†† Helmholtz Zentrum München, Neuherberg, Germany; and Division of Metabolic Diseases,§§ Technische Universität München, München, Germany

ORCID IDs: 0000-0002-5584-2366 (A-M.L.); 0000-0001-8793-9739 (A.M.F.)

Abstract Excessive circulating FAs have been proposed to promote insulin resistance (IR) of glucose metabolism by increasing the oxidation of FAs over glucose. Therefore, inhibition of FA oxidation (FAOX) has been suggested to ameliorate IR. However, prolonged inhibition of FAOX would presumably cause lipid accumulation and thereby promote lipotoxicity. To understand the glycemic consequences of acute and prolonged FAOX inhibition, we treated mice with the carnitine palmitoyltransferase 1 (CPT-1) inhibitor, etomoxir (eto), in combination with short-term 45% high fat diet feeding to increase FA availability. Eto acutely increased glucose oxidation and peripheral glucose disposal, and lowered circulating glucose, but this was associated with increased circulating FAs and triacylglycerol accumulation in the liver and heart within hours. Several days of FAOX inhibition by daily eto administration induced hepatic steatosis and glucose intolerance, specific to CPT-1 inhibition by eto. Lower whole-body insulin sensitivity was accompanied by reduction in brown adipose tissue (BAT) uncoupling protein 1 (UCP1) protein content, diminished BAT glucose clearance, and increased hepatic glucose production. Collectively, these data suggest that pharmacological inhibition of FAOX is not a viable strategy to treat IR, and that sufficient rates of FAOX are required for maintaining liver and BAT metabolic function.—Lundsgaard, A-M., A. M. Fritzen, T. S. Nicolaisen, C. S. Carl, K. A. Sjøberg, S. H. Raun, A. B. Klein, E. Sanchez-Quant, J. Langer, C. Ørskov, C. Clemmensen, M. H. Tschöp, E. A. Richter, B. Kiens, and M. Kleinert. **Glucometabolic consequences of acute and prolonged inhibition of fatty acid oxidation.** ***J. Lipid Res.*** **2020.** 61: **10–19.**

Supplementary key words carnitine palmitoyltransferase 1 • mitochondrial long-chain fatty acid import • hepatic glucose production • brown adipose tissue • liver • hyperglycemia • lipotoxicity • insulin resistance

Excess calorie intake, physical inactivity, and obesity are risk factors for developing insulin resistance (IR) and are often accompanied by an increase in circulating FAs. Several paradigms attempt to mechanistically link augmented FA availability and IR in peripheral tissues. Randle et al. (1) proposed that increased FA availability for mitochondrial

This work was supported in part by funding from the Alexander von Humboldt Foundation, the Helmholtz Alliance ICEMED, the Helmholtz Initiative on Personalized Medicine iMed by the Helmholtz Association, and the Helmholtz cross-program topic "Metabolic Dysfunction" (M.H.T.). M.K. is supported by Medical Sciences, Danish Council for Independent Research Postdoctoral Research Grant 4004-00233 and Lundbeckfonden Postdoctoral Research Grant R288-2018-78. A-M.L. and A.M.F. were supported by a postdoctoral research grant from the Danish Diabetes Academy, funded by the Novo Nordisk Foundation (NNF17SA0031406). A.M.F. was also supported by the Alfred Benzon Foundation. K.A.S. was supported by Medical Sciences, Danish Council for Independent Research Postdoctoral Research Grant 4092-00309. E.A.R. and B.K. were funded by the University of Copenhagen Excellence Program for Interdisciplinary Research (2016), "Physical Activity and Nutrition for Improvement of Health," and Medical Sciences, Danish Council for Independent Research Grant 4183-00249. C.C. receives funding from the Lundbeckfonden (Fellowship: R238-2016-2859) and the Novo Nordisk Foundation (NNF17OC0026114). The authors declare that they have no conflicts of interest with the contents of this article.

Manuscript received 3 June 2019 and in revised form 20 September 2019.

Published, JLR Papers in Press, November 12, 2019
DOI https://doi.org/10.1194/jlr.RA119000177

Abbreviations: ANGPTL8, angiopoietin-like protein 8; BAT, brown adipose tissue; BW, body weight; CD36, cluster of differentiation 36/SR-B2; CPT-1, carnitine palmitoyltransferase 1; eto, etomoxir {ethyl-2-[6-(4-chlorophenoxy)hexyl]oxirane-2-carboxylate}; eWAT, epididymal white adipose tissue; FAOX, FA oxidation; G6Pase, glucose-6-phosphatase; GLUT4, glucose transporter 4; GTT, glucose tolerance test; ^{3}H-2-DG, labeled 2-deoxyglucose; HFD, high-fat diet; iAUC, incremental area under the curve; IR, insulin resistance; LCFA, long-chain FA; LC-HFD, long-chain high-fat diet; MCFA, medium-chain FA; MC-HFD, medium-chain high-fat diet; PEPCK, phosphoenolpyruvate carboxykinase; TG, triacylglycerol; UCP1, uncoupling protein 1.

[1]To whom correspondence should be addressed.
e-mail: bkiens@nexs.ku.dk (B.K.); mkleinert@nexs.ku.dk (M.K.)

[S] The online version of this article (available at http://www.jlr.org) contains a supplement.

β-oxidation increased mitochondrial acetyl-CoA, NADH to NAD+ ratio, and citrate levels, which collectively signal to downregulate glucose oxidation and insulin-stimulated glucose disposal.

Applying this model to human IR, it has been hypothesized that augmented availability of FAs induces an increase in β-oxidation, which, by virtue of the substrate competition model, impairs glucose utilization. Therefore, it has been suggested that inhibition of FA oxidation (FAOX) should be pursued as a pharmacological strategy to improve IR by forcing increased glucose oxidation (2, 3). At the same time, IR has been shown to be accompanied by an impaired metabolic flexibility to (up)regulate FAOX in response to feeding, fasting, and exercise (4–6). This mismatch can further exacerbate IR due to the accumulation of cytosolic and intra-mitochondrial lipid metabolites (7). To this end, it seems imprudent to treat IR with pharmacological inhibition of FAOX. This conundrum exemplifies the uncertainty surrounding the question of whether inhibition of FAOX can improve glucose metabolism (8–10) or whether such a strategy would aggravate metabolic complications (11).

Carnitine palmitoyltransferase 1 (CPT-1) is one of the key enzymes for mitochondrial β-oxidation, facilitating the import of long-chain FAs (LCFAs) into the mitochondria. Located on the outer mitochondrial membrane, CPT-1 catalyzes the reaction between long-chain acyl-CoAs and carnitine to form acylcarnitine, which is then shuttled via carnitine-acylcarnitine translocase into the mitochondria, converted back into acyl-CoA (by CPT-2), and then released to undergo β-oxidation (3). We herein used the CPT-1 inhibitor, ethyl-2-[6-(4-chlorophenoxy)hexyl]oxirane-2-carboxylate [etomoxir (eto)], to inhibit FAOX in mice (12, 13) and, for the first time, compared how acute versus prolonged inhibition of FAOX impacts glucose homeostasis. Eto has been shown to inhibit CPT-1 activity in both rat heart mitochondria (14, 15), homogenates of rat heart and liver (15), and rat skeletal muscle mitochondria (16), documenting nonselectivity for CPT-1A/B isoforms and thus whole-body FAOX inhibition. To increase circulating FA availability without increasing adiposity, we provided a moderate high-fat diet (HFD) (45 E% fat) for 6 days prior to inhibition of whole-body FAOX by eto. Importantly, we also performed additional diet experiments with medium-chain FAs (MCFAs) to control for potential eto off-target effects recently described in cell-based systems (17, 18).

MATERIALS AND METHODS

Animals and diets

All animal experiments were approved by the Danish Animal Experiments Inspectorate and complied with the European convention for protection of vertebrate animals used for scientific purposes. Male C57BL/6J mice aged 14–16 weeks (Janvier Labs, France) were used for all experiments. Mice were housed on a 12 h dark-light cycle. After arrival, mice had free access to a standard rodent chow diet (Altromin #1324; Brogaarden, Denmark) and were group-housed. Two weeks prior to and during both the acute and prolonged experiments, mice were single-housed. Six days before all experiments, and also during the prolonged experiments (except for the experiment in Fig. 2), mice had ad libitum access to a moderate HFD. The diet comprised 45 kcal% fat (lard and soy bean oil) with 35 and 20 kcal% carbohydrate and protein, respectively (D01060502G; Research Diets) (also see **Table 1**). Because the fat in this diet predominantly consists of LCFAs, we hereafter refer to this diet as LC-HFD**.** In addition to this LC-HFD, we also used an additional HFD in some prolonged experiments. In this diet, the 45 kcal% fat was solely comprised of medium-chain triacylglycerol (TG) oil (caprylic and capric TG at 60% and 40%, respectively) (D18010905; Research Diets) (Table 1). The MCFA-based diet was designed to have the same energy density (kilocalories per gram) and to be isocaloric with the LC-HFD (Table 1). We hereafter refer to this diet as MC-HFD.

CPT-1 inhibitor. Eto (#1905; Sigma-Aldrich) was administered by intraperitoneal injection at 20 mg/kg body weight (BW) as in (8), diluted in 10 μl of saline per gram BW. Saline was administrated as vehicle. For all prolonged experiments, eto was administered daily at 5:00 PM, prior to the 12 h dark cycle.

Acute eto experiments in mice fed LC-HFD

Compound tolerance test. Vehicle (n = 5) or eto (n = 5) was injected in mice fasted for 5 h, and blood glucose in mixed tail blood measured with a glucometer (Contour XT; Bayer) at basal (0), 1, 2, 3, and 4 h. Mice then regained access to food, and blood glucose was measured again at 24 h.

In vivo basal glucose clearance. Vehicle (n = 9) or eto (n = 9) was injected in mice fasted for 5 h. Blood glucose was measured in mixed tail blood at basal (0). At 40 min, labeled 2-deoxyglucose (^{3}H-2-DG) (0.6 μCi/g BW) was intraperitoneally injected. Blood glucose was measured and blood obtained for ^{3}H-enrichment analyses at 50, 60, 70, and 80 min after vehicle/eto injection. Forty minutes after ^{3}H-2-DG injection, mice were euthanized by cervical decapitation. Trunk blood was obtained and tissues quickly excised [gastrocnemius muscle, heart, liver, epididymal white adipose tissue (eWAT), and brown adipose tissue (BAT)] and snap-frozen in liquid nitrogen. Two days before measurement of glucose clearance, lean and fat mass were measured by MRI-scan (EchoMIR 4-in-1; EchoMRI).

Twenty-four hour substrate oxidation. Mice (n = 12) were habituated to individual metabolic cages 3 days prior to measurement

TABLE 1. Composition of the LC-HFD and MC-HFD

	D01060502G		D18010905	
	g	*%kcal*	*g*	*%kcal*
Protein	23.7	20	23.7	20
Carbohydrate	41.4	35	41.4	35
Fat	23.6	45	23.6	45
Total	88.7	100	88.7	100
Casein	200	800	200	800
L-cystine	3	12	3	12
Corn starch	220.6	882	220.6	882
Maltodextrin 10	125	500	125	500
Sucrose	0	0	0	0
Cellulose	50	0	50	0
Soybean oil	25	225	0	0
MCT oil	0	0	202.5	1,823
Lard	177.5	1598	0	0

Besides the fat source, diets were identical in macro- and micronutrient composition. The medium-chain TG (MCT) oil was comprised of caprylic and capric acid.

and had ad libitum access to food and water at all times. Oxygen uptake and CO_2 production were measured using a calorimetric system (TSE Systems, Denmark). Glucose oxidation was calculated as 21.4 kJ/l O_2 × oxygen uptake (liters of O_2/kg BW/h) × {(100% − [(RER-0.7)/0.3]}). Data shown for the vehicle group represent basal untreated conditions. For eto, mice were intraperitoneally injected with eto at time point 3 h (10:00 AM). Mice were followed for 24 h in each condition.

Glucose tolerance. Mice were fasted at 8:00 AM. At 10:00 AM, blood glucose was measured in mixed tail blood and mice were injected with vehicle (n = 9) or eto (n = 9). At either 11:00 AM (1 h postinjection) or 2:00 PM (4 h postinjection), a glucose tolerance test (GTT) was commenced with an intraperitoneal injection of 2 g of glucose per kilogram BW and blood glucose determinations in mixed tail blood at 0, 15, 30, 60, and 120 min.

Ex vivo glucose oxidation in isolated muscle

The soleus muscle was removed from anesthetized male C57Bl/6J mice (n = 2) and mounted in an incubation reservoir (Radnoti). Muscles were bathed in 30°C Krebs-Henseleit bicarbonate buffer [5 mM glucose, 2% FA-free BSA, 0.5 mM palmitic acid (pH 7.4)] plus 50 μM of eto or DMSO as control for 20 min. The buffer was changed to fresh Krebs-Henseleit bicarbonate buffer additionally containing 512 μCi/ml [^{14}C]glucose (Amersham BioSciences, UK) plus 50 μM eto or DMSO. Following 25 min incubation, incubation medium was collected and gaseous $^{14}CO_2$ was liberated with 1 M acetic acid and trapped with vials containing 0.4 ml of benzethonium hydroxide. Radioactivity in trapped $^{14}CO_2$ was determined by liquid scintillation counting.

Prolonged FAOX inhibition with eto in mice fed either LC-HFD or MC-HFD

Sixteen mice were fed a LC-HFD and 18 mice were fed a MC-HFD (diet details in Table 1; schematic in Fig. 2A). After 6 days on the diets, half of the mice on each diet received daily intraperitoneal injections of either vehicle or eto. After 8 days of injections, a GTT (2 g/kg BW) was performed as described above the following morning (day 9). After the GTT, diet feeding and vehicle or eto intraperitoneal injections continued until day 11, and the mice were euthanized the following morning (day 12) after a 5 h fast. Liver, heart, and gastrocnemius muscle were quickly excised and snap-frozen for analysis of lipid content.

Acute-after-prolonged FAOX inhibition with eto in mice fed LC-HFD

Twenty-five mice were fed a LC-HFD (Table 1). After 6 days on the diet, mice received daily intraperitoneal injections of either vehicle (n = 9) or eto (n = 16). After 9 days of daily injections, a GTT (2 g/kg BW) was performed the next morning (day 10). For this, the mice were fasted at 8:00 AM. At 10:00 AM, blood glucose was measured in mixed tail blood and half of the eto-treated group received another injection of eto (n = 8), while the rest of the eto-treated group (n = 8) and the vehicle-treated group (n = 9) were injected with vehicle. At 2:00 PM, a GTT was conducted as described above.

Glucose-induced glucose clearance after prolonged FAOX inhibition with eto in LC-HFD-fed mice

Glucose-induced glucose clearance was evaluated in the morning after 8 days of vehicle (n = 9) or eto treatment (n = 9). After a 6 h fast, 2 g/kg BW glucose also containing ^{3}H-2-DG (0.6 μCi/g BW) were intraperitoneally injected. At 0, 15, and 30 min, glucose concentration was determined in mixed tail blood and additional blood was collected into capillary tubes. At 30 min, mice were euthanized by cervical decapitation and trunk blood was collected before tissues were collected and snap-frozen for later analyses.

Hepatic glucose production after prolonged FAOX inhibition with eto in LC-HFD-fed mice

Whole-body insulin sensitivity and endogenous glucose rate of appearance were evaluated on day 9 following 8 days of vehicle (n = 7) or eto treatment (n = 9). Mice were clamped in randomized order after a 5 h fasting period. Mice were anesthetized with an intraperitoneal injection of 11 μl/g BW of fentanyl (0.05 mg/ml; Dechra, Denmark), midazolam (5 mg/ml; Accord Healthcare, UK), and acepromazine (10 mg/ml; Pharmaxim, Sweden), and placed on a heating pad. A polyethylene cannula (PE50; Intramedic) was inserted into a jugular vein for administration of anesthetics, insulin, and glucose. Anesthesia was maintained by constant infusion of the anesthetics (0.03 μl/g). After surgery, a 60 min continuous infusion (0.83 μl/min, 1.2 μCi/h) of D-[3-^{3}H] glucose (Perkin Elmer) was administered. Then, a 120 min hyperinsulinemic-euglycemic clamp was initiated, with a primed (4.5 mU) infusion of insulin (3.8 μU insulin/kg BW/min) (Actrapid; Novo Nordisk, Denmark) and D-[3-^{3}H]glucose (0.83 μl/min, 1.2 μCi/h). Blood glucose was clamped at 6 mmol/l and maintained by variable infusion of 20% glucose solution. Blood was sampled from the tail at 105 and 120 min for determination of plasma glucose and plasma ^{3}H activity by scintillation counting to determine the plasma specific activity. At 120 min, blood for plasma insulin concentration was also obtained from the tail. Animals were euthanized by cervical dislocation.

Analyses

Plasma analyses. Plasma insulin (Alpco) and glucagon (Mercodia, Sweden) concentrations were measured by ELISA. The concentrations of plasma FA (NEFA C kit; Wako Chemicals, Denmark), TG (GPO-PAP kit; Roche Diagnostics, Denmark), and glycerol (Randox, UK) were measured colorimetrically on an autoanalyzer [Pentra C400 analyzer (Horiba, Japan)].

Tissue mRNA. Total RNA from BAT and liver was prepared using an RNeasy kit (Qiagen, Denmark). cDNA synthesis was performed with a QuantiTect reverse transcription kit (Qiagen, Denmark). Gene expression was profiled with SYBR Green-based quantitative (q)PCR, using the 7900HT Fast real-time pcr system (Thermo Fisher Scientific, Denmark). BAT and liver gene expression was normalized to hypoxanthine phosphoribosyltransferase and peptidylpropyl isomerase B, respectively. Primer sequences are given in supplemental Table S1.

Western blotting. Tissues were homogenized in ice-cold homogenization buffer, rotated end-over-end for 1 h, and lysates obtained after centrifugation at 12,000 *g* at 4°C (19). Lysates were subjected to protein determination, diluted to the same protein concentration, and subjected to SDS-PAGE and immunoblotting as described (19). The primary antibodies are described in supplemental Table S2. Bands were visualized using a Bio-Rad ChemicDoc MP imaging system (Bio-Rad). Membranes were Coomassie-stained to check for equal loading and transfer.

Tissue glycogen. Liver, heart, and skeletal muscle glycogen content was determined fluorometrically as glycosyl units after acidic hydrolysis (20).

Tissue TG. Liver TG content was measured in 20 mg of tissue as described previously (21). For heart and gastrocnemius muscle TG content, 20 mg were homogenized in 1 ml of chloroform/methanol (2:1) in a Tissuelyser II (Qiagen), then shaken for 6 h.

Three hundred microliters of water were added, and phase separation was achieved by centrifugation at 2,000 rpm for 20 min. The organic phase was isolated and dried overnight (SpeedVacPlus SC210A; Savant Instruments). TG content was measured by a colorimetric assay (#290-63701; Wako Chemicals, Denmark).

Liver histology. Tissue samples were fixed in paraformaldehyde and embedded in paraffin. Five micron sections were cut by microtome and put on glass slides. The slides were subsequently dewaxed and stained with H&E. Samples were then re-dehydrated and mounted on coverslips with Pertex. The slides were viewed in a Leitz Orthoplan microscope, and pictures were obtained using a Zeiss Axiocam ICc5 camera.

Tissue ^{3}H-2-DG uptake. Blood ^{3}H activity was measured in 5 μl of blood by scintillation counting. Ten to forty milligrams of each tissue were used to determine the accumulation of phosphorylated ^{3}H-2-DG (^{3}H-2-DG-6-P) by the precipitation method (22). Glucose clearance was calculated by dividing the tissue ^{3}H-2-DG-6-P DPM, accumulated in tissues over either 40 min (Fig. 1B) or 30 min (Fig. 4C) from tracer injection, by the average ^{3}H-2-DG DPM in blood sampled during this period (23). For the relative glucose disposal into different organs, calculations were based on lean and fat mass measured by MRI-scan. Skeletal muscle was assumed to represent 50% of the measured lean mass (24), and heart and BAT weights were assumed to be 120 mg and 200 mg, respectively, as representative for a nonobese male mouse with body mass of ∼30 g.

Statistical analyses. All data are expressed as mean ± SE. Data from Western blot analyses are presented as relative to the vehicle group. The statistical analyses performed are described in each figure legend. Statistical significance was defined as $P < 0.05$. Statistical analyses were performed in GraphPad PRISM 8 (GraphPad).

RESULTS

Acute FAOX inhibition lowers blood glucose and increases glucose oxidation and peripheral glucose clearance, while inducing systemic FA accumulation

Mice were maintained on a moderate LC-HFD for 6 days prior to eto injection. This was chosen with the aim to increase circulating FA availability without inducing confounding obesity and to replicate the protocol in a recent study investigating glucose tolerance in mice following several days of eto treatment (8). A single injection of eto (acute eto) lowered fasting blood glucose over 4 h from 8.5 to 3.1 mmol/l, with a return to normal levels 24 h later (**Fig. 1A**). Acute eto increased glucose clearance into heart, BAT, skeletal muscle, and eWAT by 22.0-, 2.6-, 2.0-, and 2.9-fold, respectively (Fig. 1B). Considering organ size, most of the glucose disposed from the blood was taken up by skeletal muscle (∼40%) and heart (∼17%) (Fig. 1C). Ex vivo incubation of soleus muscle documented an increase in glucose oxidation within skeletal muscle with acute eto (Fig. 1D). Twenty-four hour indirect calorimetry in ad libitum-fed mice revealed that whole-body glucose oxidation increased immediately following acute eto and remained elevated for 9 h (Fig. 1E). When assessed at 4 h following acute eto, where the lowering of blood glucose was pronounced, basal circulating plasma insulin and TG concentrations were unaffected, while plasma FA levels increased by 200%, but independently of increased plasma glycerol (Fig. 1F–I). Plasma glucagon was increased by 450% (Fig. 1J). At the same time, liver glycogen content was reduced by 79% with acute eto (Fig. 1K), with trends for reduction of glycogen content in both heart and skeletal muscle (Fig. 1L, M). Liver TG content was increased 400% and heart TG by 160% at 4 h, while muscle TG content remained unchanged by acute eto (Fig. 1N–P). When a GTT was conducted 1 h following eto injection, timely with the increased basal peripheral glucose clearance, the GTT incremental area under the curve (iAUC) was lowered by 53% (Fig. 1Q). When applied at 4 h following eto injection, timely with the increased plasma FAs and liver TG accumulation, the GTT iAUC was increased by 30% (Fig. 1R). Of note, the greater GTT iAUC was observed despite the findings of lower glycogen content in liver, muscle, and heart. However, absolute blood glucose levels were decreased compared with control, as basal glucose levels at the start of the GTT were 60% lower. Similar plasma insulin response during the GTT was obtained for vehicle and acute eto (Fig. 1S).

Downregulation of liver and heart but not skeletal muscle PDH-E1α Ser^{293} phosphorylation was obtained at 1 h postinjection, concomitant with the increased glucose oxidation (Fig. 1T). Collectively, these data suggest that the blood glucose lowering with acute FAOX inhibition, which can be interpreted as potentially anti-diabetic, is followed by a rise in circulating FAs, massive accumulation of liver TG, and altered glucose excursion during a GTT 4 h later.

Prolonged FAOX inhibition with eto causes glucose intolerance and hepatic TG accumulation

Given the elevated circulating FAs following acute eto, inhibition of FAOX with eto over several days (prolonged eto; schematic in **Fig. 2A**) was hypothesized to cause ectopic lipid accumulation and disrupt glucose homeostasis, independently of the last injection.

Prolonged treatment with eto did not alter food intake (supplemental Fig. S2). Importantly, to control for potential off-target effects of eto (17, 18), we took advantage of the ability of MCFAs to enter the mitochondria and undergo β-oxidation independently of the CPT-1 system (25–27). Thus, medium-chain FAOX should not be affected by eto-mediated CPT-1 inhibition. To this end, prolonged eto studies were conducted in mice fed either LC-HFD or MC-HFD (Table 1). BW was not affected by diet or treatment (supplemental Fig. S3). The MC-HFD contained medium-chain TG oil (consisting entirely of C8 and C10 MCFAs) as the only fat source. Otherwise, the MC-HFD was matched to the LC-HFD. Any effects of prolonged eto observed in mice fed the LC-HFD should not be observed in MC-HFD-fed mice.

In LC-HFD-fed mice, prolonged eto elicited an increase in fasting blood glucose and greater absolute glucose values and glucose iAUC during a GTT (Fig. 2B, C) when assessed 20 h after the last injection. In contrast, prolonged eto did not affect fasting glucose or glucose tolerance in

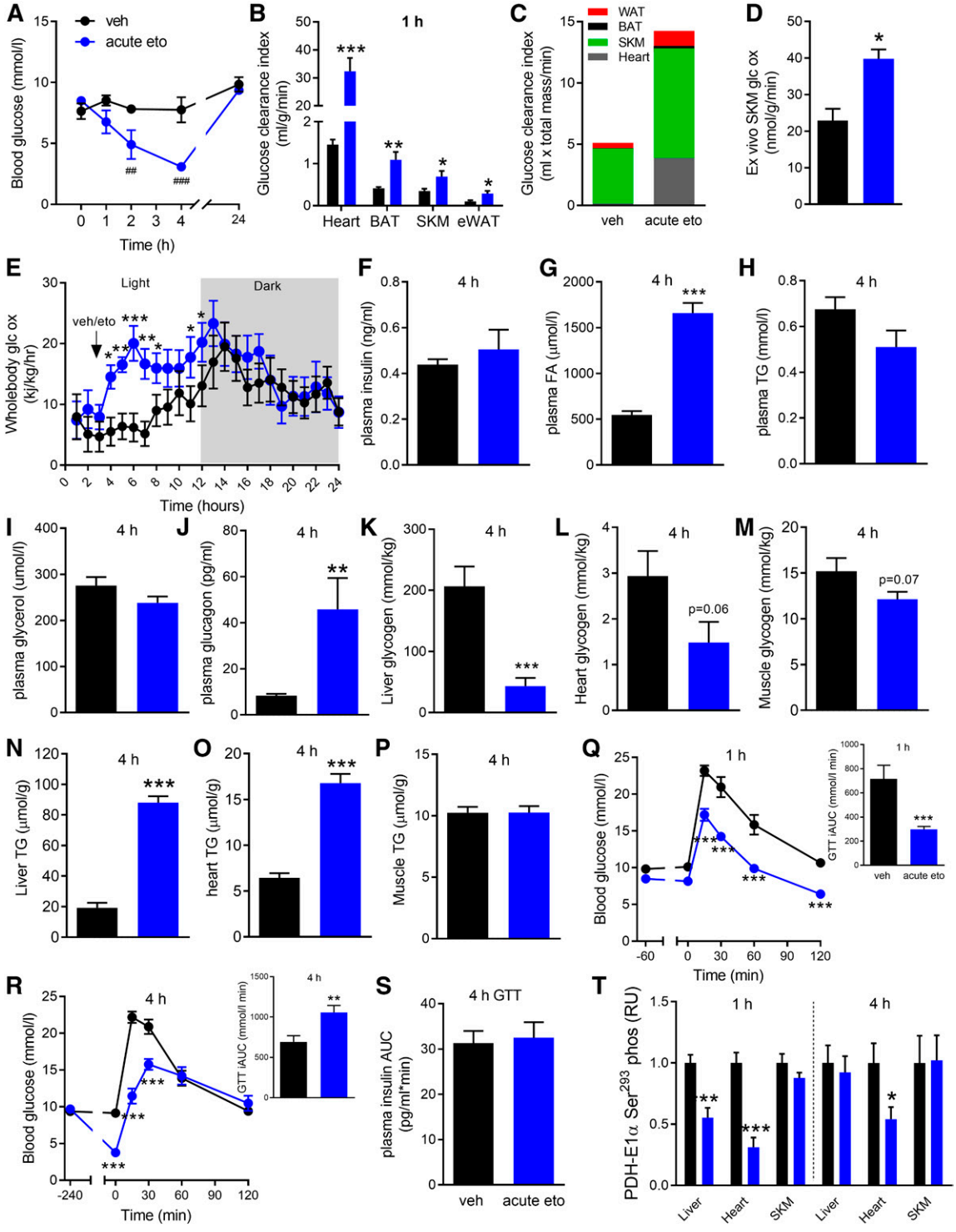

Fig. 1. Glucometabolic effects of acute FAOX inhibition. Blood glucose levels (A) at indicated time points in mice injected at 0 h with either vehicle (veh) or eto (20 mg/kg BW) (n = 5). B: Basal glucose clearance into indicated tissues (SKM, skeletal muscle) assessed between 40 to 80 min after veh or acute eto injection (n = 9). C: Glucose clearance adjusted for the estimated size of the organs (see Materials and Methods). D: Ex vivo glucose oxidation in soleus muscle incubated with veh or 50 uM eto for 45 min (n = 2). E: Whole-body glucose oxidation determined from 24 h measurements in metabolic cages (n = 12), with veh or eto injected at 3 h. For F–P, mice were injected with veh or acute eto and then euthanized at 4 h postinjection, with trunk blood and tissues collected for the indicated analyses (n = 9). GTTs (2 g glucose/kg BW) in mice fasted for 6 h, with veh or eto injection 1 h (Q) or 4 h (S) prior to GTT. iAUCs are shown (n = 8). T: PDH-E1α Ser^{293} phosphorylation in indicated tissues obtained during basal conditions at 1 h or 4 h postinjection. Representative blots are shown in supplemental Fig. S1. Data are expressed as mean ± SEM. Two-way RM ANOVA was applied in A, E, Q, and R, with Tukey's multiple comparisons post hoc test whenever interactions were detected by ANOVA. Unpaired two-tailed *t*-tests were applied in all bar graphs. ###$P < 0.001$ and ##$P < 0.01$ are differences between veh and acute eto at the indicated time point. *$P < 0.05$, **$P < 0.01$, and ***$P < 0.001$ are differences between veh and acute eto.

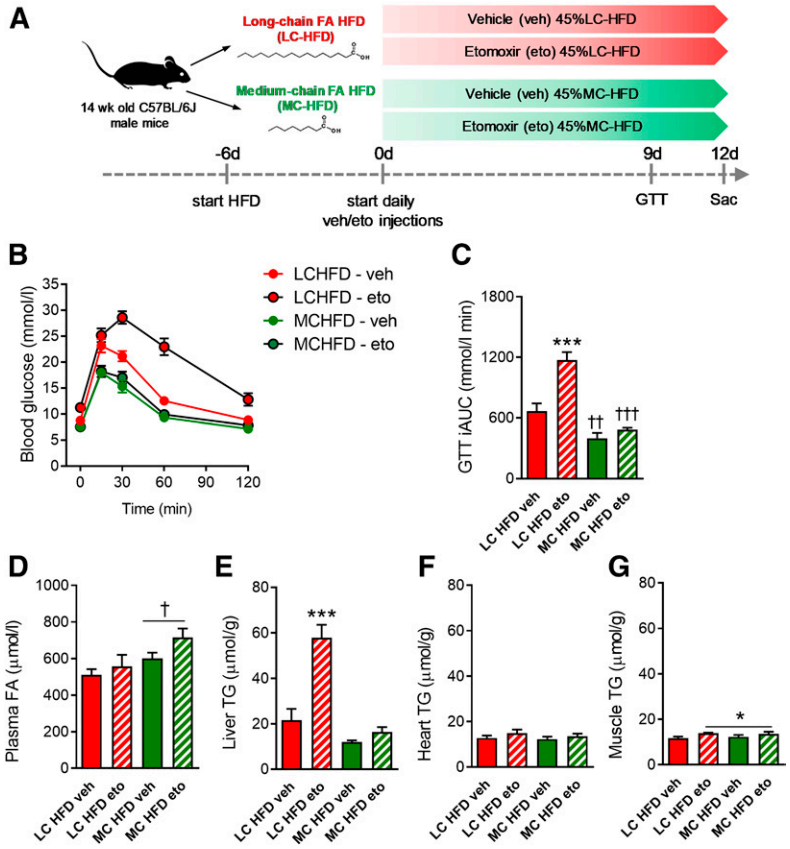

Fig. 2. Prolonged eto treatment induces glucose intolerance and hepatic lipid accumulation, effects that are specific to FAOX inhibition. A: Mice were fed either standard LC-HFD or MC-HFD for 6 days, before daily injection with either vehicle (veh) or eto (20 mg/kg BW). A GTT (2 g glucose/kg BW) was applied at day 9, with glucose excursion curves and iAUC shown in B and C. Plasma FA concentration (D) and tissue TG contents (E–G) were assessed at day 12 following euthanization. The GTT, blood sampling, and tissue excisions were performed 20 h after the last eto injection. Data are expressed as mean ± SEM. Two-way ANOVAs were applied in C–G, with Tukey's multiple comparisons test used post hoc. ***$P < 0.001$ indicates differences between veh and eto within LC-HFD. *$P < 0.05$ is a main effect of eto independently of diet. †$P < 0.05$ is a main effect of diet type. ††$P < 0.01$ and †††$P < 0.001$ indicate effect of diet within the respective intervention groups (n = 8 and n = 9 in each of the LC-HFD- and MC-HFD-fed groups, respectively).

MC-HFD-fed mice (Fig. 2B, C). Importantly, this indicates that the glucose intolerance after prolonged eto is specific to the inhibition of CPT-1 by eto and the subsequently lower availability of mitochondrial LCFAs for β-oxidation. Of note, vehicle-treated MC-HFD-fed mice were more glucose tolerant than vehicle-treated LC-HFD-fed mice (Fig. 2B, C).

Basal plasma FA concentration was not changed by prolonged eto but was increased in MC-HFD-fed mice (Fig. 2D). In LC-HFD-fed mice, prolonged eto induced a 3-fold increase in liver TG content. Importantly, there was no effect of prolonged eto on liver TG content in MC-HFD-fed mice (Fig. 2E). Heart TG was unchanged (Fig. 2F), while there was a modest (+11%) increase in skeletal muscle TG levels with prolonged eto irrespective of diet (Fig. 2G).

A recent study reported that prolonged FAOX inhibition by eto had no detrimental effect on glucose tolerance in mice (8). This interpretation depends on whether glucose tolerance is defined per absolute glucose values or the blood glucose excursion curve relative to starting value. Given the acute hypoglycemic effect of eto, we hypothesized that timing of the last eto injection would have great impact on glycemia. To test this, we assessed glucose tolerance after 9 days of eto injections, with eto last administered either 20 h (prolonged eto) or 4 h (acute-after-prolonged eto) before the GTT (**Fig. 3A**). Glucose tolerance was impaired following prolonged eto (Fig. 3B,C), in agreement with data in the prolonged experiment in Fig. 2. With acute-after-prolonged eto, the absolute blood glucose excursion was overall lower (Fig. 3B). However, relative to starting glucose levels, glucose tolerance appeared to be impaired, similar to the observation with acute eto in Fig. 1S and T.

The glucose intolerance in the prolonged eto group was observed concomitantly with normal plasma FA levels at the onset of the GTT (Fig. 3D), whereas the FA concentration was increased in the acute-after-prolonged eto group (Fig. 3D). The increased GTT iAUC following acute-after-prolonged eto was observed despite depletion of liver glycogen and 29% reduction of muscle glycogen levels in the basal state (Fig. 3E, F).

Collectively, these results indicate that longer-term inhibition of FAOX by eto impairs glucose tolerance and increases ectopic lipid accumulation in the liver. The glucose intolerance was not reversed by acute inhibition of FAOX.

Prolonged FAOX inhibition with eto impairs hepatic and BAT insulin sensitivity

Next, we wanted to understand whether the glucose intolerance after prolonged eto is secondary to impairments in peripheral insulin sensitivity or insulin secretion. Following injection with glucose, plasma glucose levels were 36% higher at 30 min in prolonged eto mice compared with vehicle (**Fig. 4A**). Both groups, however, exhibited a similar increase in circulating insulin (Fig. 4B), indicating that insulin secretion is unaffected by prolonged eto. Glucose-induced glucose clearance into skeletal muscle, heart, and eWAT was similar in both groups, but prolonged eto decreased glucose clearance into the BAT by 48% (Fig. 4C). Glucose-induced Akt Thr^{308} phosphorylation was not impaired in BAT, skeletal muscle, or liver following prolonged

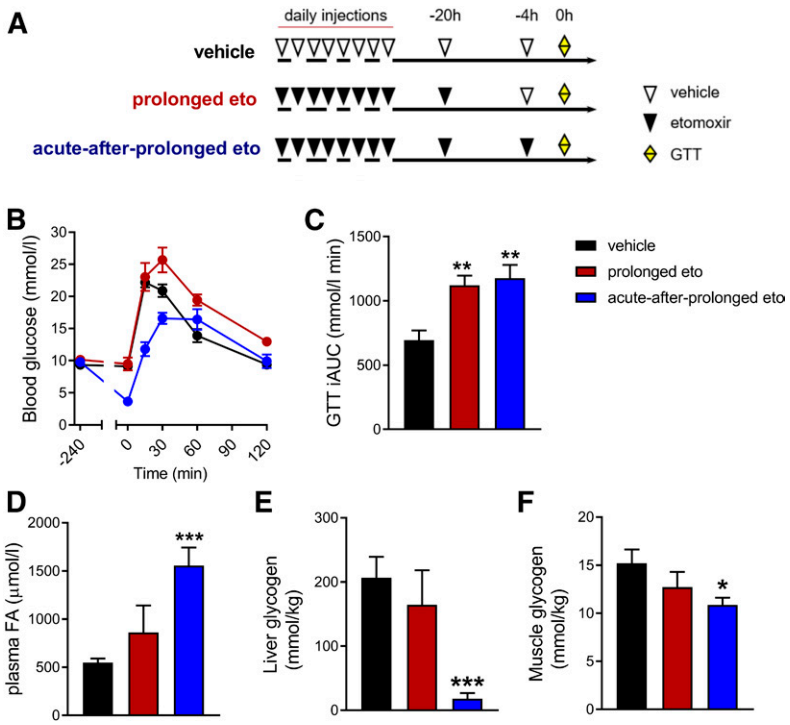

Fig. 3. Timing of last eto injection influences glucose tolerance following prolonged inhibition of FAOX. Mice were fed a LC-HFD for 6 days before daily intraperitoneal injections with either vehicle or eto (20 mg/kg BW) for 9 days (A). The next day a GTT (2 g glucose per kilogram BW) was performed. Four hours prior to the start of the GTT, blood was collected from the tail and mice in the vehicle and prolonged eto groups received an injection of vehicle, while mice in the acute-after-prolonged eto group were injected with eto (A). Glucose excursion curves (B) and iAUC (C). For D and E, mice were treated similar to (A), but mice were euthanized before the GTT and 6 h fasted plasma FA concentration (D), glycogen content in liver (E), and skeletal muscle (F) were obtained. Data are expressed as mean ± SEM. One-way ANOVAs were applied in C–F. *** $P < 0.001$, ** $P < 0.01$, and * $P < 0.05$ are differences compared with the vehicle group(n = 9 mice in veh, n = 8 mice in prolonged and acute-after-prolonged eto).

eto (Fig. 4D). In BAT, a decreased protein content of glucose transporter 4 (GLUT4) was observed, together with decreased uncoupling protein 1 (UCP1) protein and mitochondrial complex I–V (Fig. 4E). In agreement with a dysregulation of BAT metabolism, lower mRNA content was detected for UCP1, cytochrome C1 (Cyc1), and PR domain containing 16 (Prdm16) with prolonged eto (Fig. 4G), while these browning genes remained unaltered in BAT from prolonged eto MC-HFD-fed mice (Fig. 4H). Visually, BAT excised from prolonged eto-treated LC-HFD-fed mice showed a more beige phenotype (supplemental Fig. S5).

In addition to a defect in BAT glucose clearance, the elevation in hepatic TG content after prolonged eto (Fig. 2E) indicated that defects in liver glucose metabolism might also contribute to the glucose intolerance. To understand whether hepatic glucose output was affected by prolonged eto, a hyperinsulinemic-euglycemic clamp was conducted. Plasma insulin and blood glucose (clamped at ∼6 mmol/l) were similar during the clamp in the vehicle and prolonged eto groups (**Fig. 5A**, B). A reduction in the glucose infusion rate was detected following prolonged eto (Fig. 5C), and this was accompanied by increased hepatic glucose production (Fig. 5D). After the clamp, liver

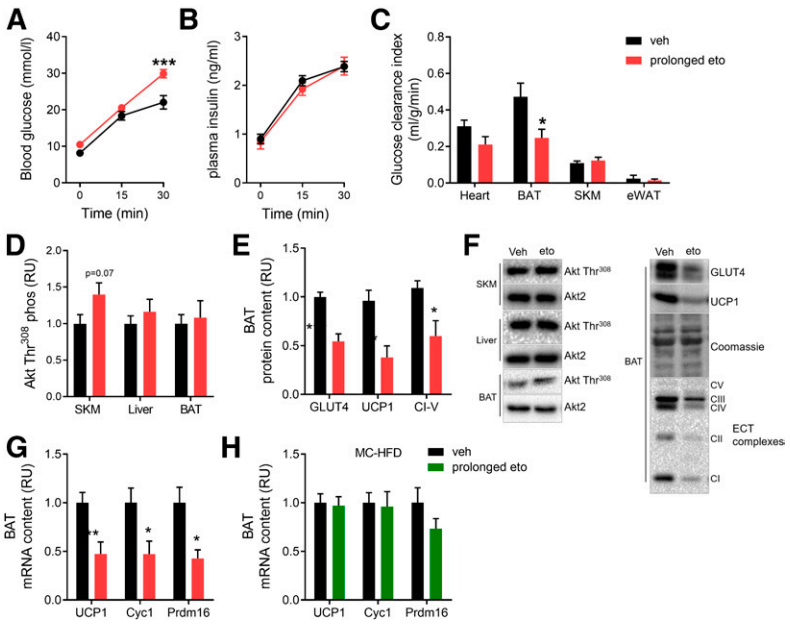

Fig. 4. Prolonged FAOX inhibition impairs glucose-induced glucose disposal in BAT. Glucose-induced glucose disposal was evaluated in mice subjected to prolonged FAOX inhibition, with the last vehicle (veh) or eto injection 20 h before the experiment. Blood glucose (A) and plasma insulin (B) levels at indicated time-points after intraperitoneal injection with glucose (2g/kg BW) with ^{3}H-2-DG at time point 0. Glucose-stimulated glucose clearance into indicated tissues (C) (SKM, skeletal muscle). D: Akt Thr^{308} phosphorylation evaluated in SKM, liver, and BAT 30 min following glucose injection. E: Protein expression of indicated proteins after prolonged eto treatment in BAT from mice fed the LC-HFD. F: Representative blots to D and E. G, H: Gene expression of indicated genes after prolonged eto treatment in BAT from mice fed LC-HFD (G) as in A–E, or MC-HFD (H). Data are expressed as mean ± SEM. Two-way RM ANOVAs were applied in A and B. Unpaired *t*-tests were applied in C–E, G, and H. ***$P < 0.001$, **$P < 0.01$, and *$P < 0.05$ are differences compared with the vehicle group. In A–C, n = 9 in each group. In D–H, n = 9 mice in veh and n = 9 mice in prolonged eto. Cyc1, cytochrome C1; Prdm16, PR domain containing 16.

glycogen content was not lower in prolonged eto mice (Fig. 5E). It could thus be speculated that hepatic gluconeogenesis, rather than increased hepatic glycogenolysis, contributed to the increased glucose output from the liver. Histology of liver sections revealed no gross morphological signs of hepatic fibrosis in livers after prolonged eto (Fig. 5F). Fasting plasma TG was nonsignificantly increased by 85% with prolonged eto (Fig. 5G). Hepatic protein and gene expression analyses showed an increase in the protein content of cluster of differentiation 36/SR-B2 (CD36) (+50%), a key enzyme for FA uptake (Fig. 5H). As phosphoenolpyruvate carboxykinase (PEPCK) protein content was increased (+81%), together with increased glucose-6-phosphatase (G6Pase) mRNA (+65%) and diminished angiopoietin-like protein 8 (ANGPTL8) mRNA (−68%) (Fig. 5H, I), this could indicate a greater hepatic gluconeogenic capacity of the liver after prolonged eto. Expression of hepatic FAOX genes, such as PPARα, PDK4, and CPT-1α, were not significantly changed. Collectively, these data suggest that the lower glucose tolerance following prolonged FAOX inhibition is a consequence of IR in the liver and BAT.

DISCUSSION

We show that inhibiting long-chain FAOX with eto initially lowers basal blood glucose levels and increases whole-body and skeletal muscle glucose oxidation, increases peripheral glucose disposal in several oxidative tissues, and leads to an initial reduction in blood glucose excursion following a GTT. The lowering of basal blood glucose is, however, accompanied by a substantial rise in circulating FAs, accumulation of TG in liver and heart, and hours later a reduced glucose tolerance relative to starting glucose levels. Furthermore, when FAOX is inhibited over several days, severe metabolic dysfunctions manifest specifically in liver and BAT, causing whole body IR. Importantly, using a control diet, we verify that these findings directly relate to the lack of mitochondrial oxidation of FAs and not to possible unspecific effects of eto.

Our observation that acute FAOX inhibition lowered basal blood glucose levels is consistent with previous studies in rodents (28–30) and humans (3, 9, 31, 32). However, our data provide new important insights. First, we for the first time traced glucose clearance by several key metabolic tissues that contribute to whole-body glucose homeostasis and found that cardiac glucose disposal was robustly increased by acute FAOX inhibition, likely related to FAs being a major substrate for heart energy production (33). Compared with the heart, glucose disposal into skeletal muscle was induced to a lesser extent, with glucose clearance increasing 2-fold following acute FAOX inhibition. However, this 2-fold increase in muscle glucose clearance is similar to the effect of physiological insulin stimulation in mouse muscle in vivo (34); and taking organ size into consideration, most of the systemic glucose was presumably taken up by skeletal muscle. At the same time, it was shown in isolated skeletal muscle that incubation with eto acutely increased glucose oxidation. Second, efficient disposal of glucose during a GTT was initially increased, while being reduced 4 h later following acute inhibition of FAOX. Thus, the lowering of glycemia with acute FAOX inhibition by eto appears to be associated with a later onset of altered glucose homeostatic control. A potential mechanism for the greater relative glucose excursions during the GTT after 4 h of acute eto is the concomitant rise in circulating

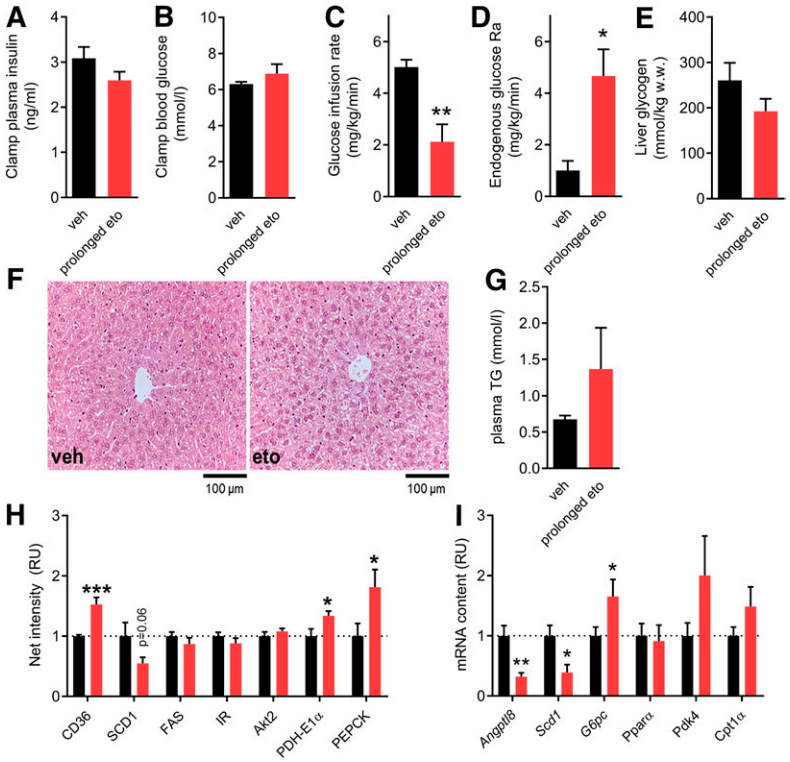

Fig. 5. Prolonged FAOX inhibition results in increased hepatic glucose production under insulin stimulation. Insulin-stimulated whole-body glucose disposal and glucose production assessed during a 120 min hyperinsulinemic-euglycemic clamp combined with D-[3-^{3}H]glucose infusion. Experiments were performed in mice subjected to prolonged FAOX inhibition, with the last vehicle (veh) or eto injection 20 h before the experiment. Average plasma insulin (A), glucose (B), and glucose infusion rate required to maintain euglycemia (C) during the last 30 min of the clamp. The glucose rate of appearance (Ra) (D) obtained at 105 and 120 min. Liver glycogen content obtained at 120 min in the clamp experiment is shown in E. F: Representative images of H&E-stained liver sections. G: Fasting plasma TG after prolonged inhibition of FAOX, with the last vehicle (veh) or eto injection 20 h before the experiment. Quantification of indicated liver protein contents (H). Representative blots are shown in supplemental Fig. S4. I: Hepatic mRNA content for indicated genes. Data are expressed as mean ± SEM. Unpaired *t*-tests were applied in A–E and G–I. ***$P < 0.001$, **$P < 0.01$, and *$P < 0.05$ are differences compared with the vehicle group. In A–E, n = 7 mice in veh, n = 9 mice in prolonged eto. In G–I, n = 9 mice in veh, n = 9 mice in prolonged eto. RU, relative units.

FAs (13), likely related to the suppression of whole-body FAOX with acute eto, as plasma glycerol levels did not indicate increased whole-body lipolysis. According to Randle's findings, high systemic FA availability can acutely downregulate insulin-stimulated glucose disposal (1, 35). Associated with the increased plasma FA levels, hepatic TG content was 4-fold increased, and it could be speculated whether increased hepatic glucose output during the 4 h GTT contributed to the greater GTT iAUC, similar to after prolonged eto. Glucagon was markedly increased at 4 h, likely induced by the marked hypoglycemia at that time point rather than direct effects of eto on α-cells (36). Together, the initial whole-body response to eto administration highlights potential metabolic concerns regarding the use of pharmacological FAOX inhibition to treat hyperglycemia in diabetes.

The glycemic consequences of longer-term pharmacological FAOX inhibition were previously contradictory. Rats treated with eto for a prolonged period were reported to be insulin resistant (11). In contrast, prolonged FAOX inhibition in mice lowered the absolute glucose concentrations during a GTT despite elevated concentrations of skeletal muscle diacylglycerols (8). The present data show that the findings by Timmers et al. (8) likely related to the fact that eto in that study was administrated a few hours prior to the GTT.

In our study, prolonged FAOX inhibition by eto caused glucose intolerance by inducing IR in both liver and BAT. The dysregulation of hepatic glucose production was related to an increase in hepatic TG content and a progluconeogenic molecular signature. Hepatic TG accumulation possibly resulted from the intermittent inhibitions of hepatic FAOX after the daily eto injections, concomitant with the intermittent increases in plasma FA availability resulting from peripheral FAOX inhibition coupled with a compensatory upregulation of the FA translocase, CD36, in the liver over time. Of note, humans with carnitine deficiency, which impairs the function of the CPT shuttle, also demonstrate hepatic TG accumulation (37, 38). Moreover, when eto was administered to obese insulin-resistant subjects for 3 days, the fasting concentration of plasma FAs increased by 52% (3). Following prolonged FAOX inhibition, we here show that protein content of PEPCK, an enzyme facilitating the first committed step in gluconeogenesis (39), was increased, while mRNA content of ANGPTL8, with suppressing effects on gluconeogenic gene transcription (40), was decreased. Together with an increased G6Pase mRNA content, these data support that prolonged inhibition of FAOX increases the capacity for hepatic glucose output.

The observed IR in the BAT was not associated with defective insulin signaling as judged by Akt Thr^{308} phosphorylation, and seems rather to be related to the marked downregulation of GLUT4 content and the impaired oxidative/uncoupling capacity. In BAT, we made the observation of a decrease in UCP1 protein content following prolonged FAOX inhibition. It has been shown that LCFAs are essential to activate UCP1 (41, 42), and that BAT thermogenic function and UCP1 expression were impaired in the absence of LCFAs (43–45). To this end, reducing LCFA availability by administration of the whole-body lipolysis inhibitor, nicotinic acid, in humans suppressed cold-induced BAT thermogenesis (46). Sufficient FAOX thus appears to be necessary for normal BAT function. As thermogenic gene expression and BAT morphology remained normal when eto was administered in MC-HFD-fed mice, this indicates that the metabolic deterioration of BAT was specific to mitochondrial FA availability and β-oxidation.

In conclusion, we show that acute inhibition of FAOX reduces glucose tolerance relative to starting levels after a few hours, and that prolonged FAOX inhibition induces both glucose intolerance and IR. While acute inhibition of FAOX actually lowers blood glucose, due to increased glucose utilization primarily in skeletal muscle and the heart, the accompanying increase in circulating FAs (and the resulting liver TG accumulation) was likely the reason for the altered glucose tolerance observed 4 h into FAOX inhibition. Prolonged inhibition of FAOX led to IR in liver and BAT, independently of a concomitant increase in circulating FA levels, pointing to intrinsic tissue metabolic dysregulation. Impaired hepatic glucoregulation seemed to be an important mechanism for the impaired glucose homeostasis. Collectively, our data suggest that pharmacological FAOX inhibition, despite the transient stimulation of glucose oxidation, does not appear to be a viable strategy to treat IR.

Novo Nordisk Foundation Center for Basic Metabolic Research is an independent research center based at the University of Copenhagen, Denmark, and is partially funded by an unconditional donation from the Novo Nordisk Foundation.

REFERENCES

1. Randle, P. J., P. B. Garland, C. N. Hales, and E. A. Newholme. 1963. The glucose fatty-acid cycle. Its role in insulin sensitivity and the metabolic disturbances of diabetes mellitus. *Lancet.* **1:** 785–789.
2. Zhang, L., W. Keung, V. Samokhvalov, W. Wang, and G. D. Lopaschuk. 2010. Role of fatty acid uptake and fatty acid beta-oxidation in mediating insulin resistance in heart and skeletal muscle. *Biochim. Biophys. Acta.* **1801:** 1–22.
3. Ratheiser, K., B. Schneeweiss, W. Waldhausl, P. Fasching, A. Korn, P. Nowotny, M. Rohac, and H. P. Wolf. 1991. Inhibition by etomoxir of carnitine palmitoyltransferase I reduces hepatic glucose production and plasma lipids in non-insulin-dependent diabetes mellitus. *Metabolism.* **40:** 1185–1190.
4. Felber, J. P., E. Ferrannini, A. Golay, H. U. Meyer, D. Theibaud, B. Curchod, E. Maeder, E. Jequier, and R. A. DeFronzo. 1987. Role of lipid oxidation in pathogenesis of insulin resistance of obesity and type II diabetes. *Diabetes.* **36:** 1341–1350.
5. Kelley, D. E., B. Goodpaster, R. R. Wing, and J. A. Simoneau. 1999. Skeletal muscle fatty acid metabolism in association with insulin resistance, obesity, and weight loss. *Am. J. Physiol.* **277:** E1130–E1141.
6. Blaak, E. E. 2004. Basic disturbances in skeletal muscle fatty acid metabolism in obesity and type 2 diabetes mellitus. *Proc. Nutr. Soc.* **63:** 323–330.
7. Koves, T. R., J. R. Ussher, R. C. Noland, D. Slentz, M. Mosedale, O. Ilkayeva, J. Bain, R. Stevens, J. R. Dyck, C. B. Newgard, et al. 2008. Mitochondrial overload and incomplete fatty acid oxidation contribute to skeletal muscle insulin resistance. *Cell Metab.* **7:** 45–56.
8. Timmers, S., M. Nabben, M. Bosma, B. van Bree, E. Lenaers, D. van Beurden, G. Schaart, M. S. Westerterp-Plantenga, W. Langhans, M. K. Hesselink, et al. 2012. Augmenting muscle diacylglycerol and triacylglycerol content by blocking fatty acid oxidation does not impede insulin sensitivity. *Proc. Natl. Acad. Sci. USA.* **109:** 11711–11716.

9. Hübinger, A., O. Knode, F. Susanto, R. Reinauer, and F. A. Gries. 1997. Effects of the carnitine-acyltransferase inhibitor etomoxir on insulin sensitivity, energy expenditure and substrate oxidation in NIDDM. *Horm. Metab. Res.* **29:** 436–439.
10. Keung, W., J. R. Ussher, J. S. Jaswal, M. Raubenheimer, V. H. Lam, C. S. Wagg, and G. D. Lopaschuk. 2013. Inhibition of carnitine palmitoyltransferase-1 activity alleviates insulin resistance in diet-induced obese mice. *Diabetes.* **62:** 711–720.
11. Dobbins, R. L., L. S. Szczepaniak, B. Bentley, V. Esser, J. Myhill, and J. D. McGarry. 2001. Prolonged inhibition of muscle carnitine palmitoyltransferase-1 promotes intramyocellular lipid accumulation and insulin resistance in rats. *Diabetes.* **50:** 123–130.
12. Ceccarelli, S. M., O. Chomienne, M. Gubler, and A. Arduini. 2011. Carnitine palmitoyltransferase (CPT) modulators: a medicinal chemistry perspective on 35 years of research. *J. Med. Chem.* **54:** 3109–3152.
13. Schönke, M., J. Massart, and J. R. Zierath. 2018. Effects of high-fat diet and AMPK modulation on the regulation of whole-body lipid metabolism. *J. Lipid Res.* **59:** 1276–1282.
14. Lilly, K., C. Chung, J. Kerner, R. VanRenterghem, and L. L. Bieber. 1992. Effect of etomoxiryl-CoA on different carnitine acyltransferases. *Biochem. Pharmacol.* **43:** 353–361.
15. Declercq, P. E., J. R. Falck, M. Kuwajima, H. Tyminski, D. W. Foster, and J. R. McGarry. 1987. Characterization of the mitochondrial carnitine palmitoyltransferase enzyme system. I. Use of inhibitors. *J. Biol. Chem.* **262:** 9812–9821.
16. Luiken, J. J., H. E. Niessen, S. L. Coort, N. Hoebers, W. A. Coumans, R. W. Schwenk, A. Bonen, and J. F. Glatz. 2009. Etomoxir-induced partial carnitine palmitoyltransferase-I (CPT-I) inhibition in vivo does not alter cardiac long-chain fatty acid uptake and oxidation rates. *Biochem. J.* **419:** 447–455.
17. Divakaruni, A. S., W. Y. Hsieh, L. Minarrieta, R. N. Duong, K. K. O. Kim, B. R. Desousa, A. Y. Andreyev, C. E. Bowman, K. Caradonna, B. P. Dranka, et al. 2018. Etomoxir inhibits macrophage polarization by disrupting CoA homeostasis. *Cell Metab.* **28:** 490–503.e7.
18. Kajihara, N., D. Kukidome, K. Sada, H. Motoshima, N. Furukawa, T. Matsumura, T. Nishikawa, and E. Araki. 2017. Low glucose induces mitochondrial reactive oxygen species via fatty acid oxidation in bovine aortic endothelial cells. *J. Diabetes Investig.* **8:** 750–761.
19. Kleinert, M., B. L. Parker, A. M. Fritzen, J. R. Knudsen, T. E. Jensen, R. Kjobsted, L. Sylow, M. Ruegg, D. E. James, and E. A. Richter. 2017. Mammalian target of rapamycin complex 2 regulates muscle glucose uptake during exercise in mice. *J. Physiol.* **595:** 4845–4855.
20. Passonneau, J. V., P. D. Gatfield, D. W. Schulz, and O. H. Lowry. 1967. An enzymic method for measurement of glycogen. *Anal. Biochem.* **19:** 315–326.
21. Lundsgaard, A. M., J. B. Holm, K. A. Sjoberg, K. N. Bojsen-Moller, L. S. Myrmel, E. Fjaere, B. A. H. Jensen, T. S. Nicolaisen, J. R. Hingst, S. L. Hansen, et al. 2019. Mechanisms preserving insulin action during high dietary fat intake. *Cell Metab.* **29:** 50–63.e4.
22. Ferré, P., A. Leturque, A. F. Burnol, L. Penicaud, and J. Girard. 1985. A method to quantify glucose utilization in vivo in skeletal muscle and white adipose tissue of the anaesthetized rat. *Biochem. J.* **228:** 103–110.
23. Fazakerley, D. J., A. M. Fritzen, M. E. Nelson, I. H. Thorius, K. C. Cooke, S. J. Humphrey, G. J. Cooney, and D. E. James. 2019. Insulin tolerance test under anaesthesia to measure tissue-specific insulin-stimulated glucose disposal. *Bio Protoc.* **9:** doi:10.21769/BioProtoc.3146.
24. Rolfe, D. F., and G. C. Brown. 1997. Cellular energy utilization and molecular origin of standard metabolic rate in mammals. *Physiol. Rev.* **77:** 731–758.
25. Irie, H., I. B. Krukenkamp, J. F. Brinkmann, G. R. Gaudette, A. E. Saltman, W. Jou, J. F. Glatz, N. A. Abumrad, and A. Ibrahimi. 2003. Myocardial recovery from ischemia is impaired in CD36-null mice and restored by myocyte CD36 expression or medium-chain fatty acids. *Proc. Natl. Acad. Sci. USA.* **100:** 6819–6824.
26. Schönfeld, P., and L. Wojtczak. 2016. Short- and medium-chain fatty acids in energy metabolism: the cellular perspective. *J. Lipid Res.* **57:** 943–954.
27. Violante, S., L. Ijlst, B. H. Te, J. Koster, A. I. Tavares, R. J. Wanders, F. V. Ventura, and S. M. Houten. 2013. Peroxisomes contribute to the acylcarnitine production when the carnitine shuttle is deficient. *Biochim. Biophys. Acta.* **1831:** 1467–1474.
28. Reaven, G. M., H. Chang, and B. B. Hoffman. 1988. Additive hypoglycemic effects of drugs that modify free-fatty acid metabolism by different mechanisms in rats with streptozocin-induced diabetes. *Diabetes.* **37:** 28–32.
29. Swislocki, A., and T. Eason. 1994. Glucose tolerance and blood pressure are improved in the spontaneously hypertensive rat by ethyl-2-(6-(4-chlorophenoxy)-hexyl)oxirane-2-carboxylate (etomoxir), an inhibitor of fatty acid oxidation. *Am. J. Hypertens.* **7:** 739–744.
30. Kruszynska, Y. T., and H. S. Sherratt. 1987. Glucose kinetics during acute and chronic treatment of rats with 2[6(4-chlorophenoxy)hexyl]oxirane-2-carboxylate, etomoxir. *Biochem. Pharmacol.* **36:** 3917–3921.
31. Hinderling, V. B., P. Schrauwen, W. Langhans, and M. S. Westerterp-Plantenga. 2002. The effect of etomoxir on 24-h substrate oxidation and satiety in humans. *Am. J. Clin. Nutr.* **76:** 141–147.
32. Schrauwen, P., V. Hinderling, M. K. Hesselink, G. Schaart, E. Kornips, W. H. Saris, M. Westerterp-Plantenga, and W. Langhans. 2002. Etomoxir-induced increase in UCP3 supports a role of uncoupling protein 3 as a mitochondrial fatty acid anion exporter. *FASEB J.* **16:** 1688–1690.
33. Bing, R. J., A. Siegel, I. Ungar, and M. Gilbert. 1954. Metabolism of the human heart. II. Studies on fat, ketone and amino acid metabolism. *Am. J. Med.* **16:** 504–515.
34. Kleinert, M., L. Sylow, D. J. Fazakerley, J. R. Krycer, K. C. Thomas, A. J. Oxboll, A. B. Jordy, T. E. Jensen, G. Yang, P. Schjerling, et al. 2014. Acute mTOR inhibition induces insulin resistance and alters substrate utilization in vivo. *Mol. Metab.* **3:** 630–641.
35. Høeg, L. D., K. A. Sjoberg, J. Jeppesen, T. E. Jensen, C. Frosig, J. B. Birk, B. Bisiani, N. Hiscock, H. Pilegaard, J. F. Wojtaszewski, et al. 2011. Lipid-induced insulin resistance affects women less than men and is not accompanied by inflammation or impaired proximal insulin signaling. *Diabetes.* **60:** 64–73.
36. Hong, J., P. B. Jeppesen, I. Nordentoft, and K. Hermansen. 2007. Fatty acid-induced effect on glucagon secretion is mediated via fatty acid oxidation. *Diabetes Metab. Res. Rev.* **23:** 202–210.
37. Longo, N., M. Frigeni, and M. Pasquali. 2016. Carnitine transport and fatty acid oxidation. *Biochim. Biophys. Acta.* **1863:** 2422–2435.
38. Gilbert, E. F. 1985. Carnitine deficiency. *Pathology.* **17:** 161–171.
39. Hanson, R. W. 2009. Thematic minireview series: a perspective on the biology of phosphoenolpyruvate carboxykinase 55 years after its discovery. *J. Biol. Chem.* **284:** 27021–27023.
40. Rong Guo, X., W. X. Li, Y. Chen, Y. Y. Hong, C. Y. Mei, Y. Ding, J. Fang, B. L. Jiao, and L. D. Sheng. 2016. ANGPTL8/betatrophin alleviates insulin resistance via the Akt-GSK3beta or Akt-FoxO1 pathway in HepG2 cells. *Exp. Cell Res.* **345:** 158–167.
41. Fedorenko, A., P. V. Lishko, and Y. Kirichok. 2012. Mechanism of fatty-acid-dependent UCP1 uncoupling in brown fat mitochondria. *Cell.* **151:** 400–413.
42. Heaton, G. M., and D. G. Nicholis. 1976. Hamster brown-adipose-tissue mitochondria. The role of fatty acids in the control of the proton conductance of the inner membrane. *Eur. J. Biochem.* **67:** 511–517.
43. Shin, H., Y. Ma, T. Chanturiya, Q. Cao, Y. Wang, A. K. G. Kadegowda, R. Jackson, D. Rumore, B. Xue, H. Shi, et al. 2017. Lipolysis in brown adipocytes is not essential for cold-induced thermogenesis in mice. *Cell Metab.* **26:** 764–777.e5.
44. Lee, J., J. M. Ellis, and M. J. Wolfgang. 2015. Adipose fatty acid oxidation is required for thermogenesis and potentiates oxidative stress-induced inflammation. *Cell Reports.* **10:** 266–279.
45. Gonzalez-Hurtado, E., J. Lee, J. Choi, and M. J. Wolfgang. 2018. Fatty acid oxidation is required for active and quiescent brown adipose tissue maintenance and thermogenic programing. *Mol. Metab.* **7:** 45–56.
46. Blondin, D. P., F. Frisch, S. Phoenix, B. Guerin, E. E. Turcotte, F. Haman, D. Richard, and A. C. Carpentier. 2017. Inhibition of intracellular triglyceride lipolysis suppresses cold-induced brown adipose tissue metabolism and increases shivering in humans. *Cell Metab.* **25:** 438–447.